Structures of $C_nH_x^+$ Molecules for $n \leq 22$ and $x \leq 5$: Emergence of PAHs and Effects of Dangling Bonds on Conformation

Seonghoon Lee, Nigel Gotts, Gert von Helden, and Michael T. Bowers*

Department of Chemistry, University of California at Santa Barbara, Santa Barbara, California 93106-9510

Received: October 14, 1996; In Final Form: January 7, 1997[⊗]

Mixed carbon/hydrogen cationic clusters, $C_nH_x^+$ are generated in a laser desorption ion source over the size range $0 \leq x \leq 5$ and $5 \leq n \leq 22$. These species are mass selected and their conformations determined using ion mobility/ion chromatography methods. The conformations of pure carbon cationic species have been previously reported as pure linear chains for $n \leq 6$, mixed chains and monocyclic rings for $7 \leq n \leq 9$, and pure monocyclic rings for $n \geq 10$. Addition of a single H atom extends the range of linear species to $n = 15$, and addition of two or more H atoms extends the linear isomer to $n \geq 22$, primarily at the expense of the fraction of monocyclic ring present. At $n = 15$ a new isomer appears for $x \geq 4$ and persists to $n \geq 22$. Evidence is presented that this isomer is most likely a benzene ring with a carbon loop attached at ortho positions, providing a starting point for polycyclic aromatic hydrocarbon (PAH) formation in carbon/hydrogen plasmas. The fraction of linear isomer for $C_nH_2^+$ is ∼1.0 up to $n = 12$ and then smoothly decreases relative to the monocyclic isomer until it is nearly gone at $n = 20$. This fractional abundance is quantitatively matched by C_n^- anions over this range of n, indicating H atoms act primarily as electron donors tying up dangling bonds. This analogy indicates C_nH^+ abundances should then reflect C_n abundances, quantities that cannot be directly measured experimentally. The C_nH^+ relative linear isomer abundances fall between C_n^+ and C_n^- (or $C_nH_2^+$) abundances, declining from 1.0 at $n = 8$ to near 0.0 at $n = 16$, indicating large linear carbon clusters are almost certainly unstable to ring closure.

Introduction

Carbon is the most versatile, ubiquitous element, and as such, its chemistry and the chemistry of its clusters have been of interest for many years.[1] In the past decade, however, this interest has greatly intensified following the discovery of the hollow cage fullerene carbon compounds[2] and the ability to separate certain of them in macroscopic quantities.[3] Research is exploding in the carbon material area, especially in the generation of carbon tubules[4] and in metallocarbon composite materials.[5] These species lend themselves to characterization by traditional spectroscopic methods and newer surface-sensitive techniques like scanning tunneling microscopy.

To date, there have been no reports of bulk isolation of pure carbon clusters with sizes below C_{60}. As a consequence, investigating these smaller systems is a tremendous challenge, and rather exotic methods must be employed. In addition, the measurements must be made either in the gas phase or in dilute, inert matrices due to the very high chemical reactivity of pure carbon clusters. This reactivity comes from unfulfilled dangling bonds and/or from strain energy in the pure carbon species formed to minimize dangling bonds.

One method that has proven to be quite effective in studying the smaller carbon clusters is the ion mobility-based method termed ion chromatography (IC).[6] In this method accurate collision cross sections of mass-selected carbon clusters are obtained. These cross sections are then compared to cross sections of model structures, and in almost all cases unambiguous structural confirmation of a given species can be obtained.[6,7] The method has been successfully applied to carbon clusters over the range C_5 to C_{80} for both positive[8] and negative[9] ions. Of importance is the fact that identical "families" of structures were obtained for both the cations and anions, although the range of stability for a given family did vary with charge state. It was found that small systems formed linear chains. Around C_{10} monocyclic rings appeared and soon dominated. A sequence of families of large planar ring systems followed with bicyclic rings appearing near C_{20}, tricyclic near C_{30}, and so on. For positive ions the first fullerene appeared at C_{30}^+, and by C_{50}^+ fullerenes were the dominant structure.[8] Interestingly, for negative ions fullerenes comprised a very minor isomeric percentage (<10%) until C_{60}^-, where the fullerene represented ∼20% of the C_{60}^- composition. Large planar rings were the dominant species for the anions.[9b]

One family of structures was notably absent. This family contained the curved, or bowl-shaped, five- and six-member ring species that were initially presumed to form the building blocks of fullerenes.[10] It was imagined that carbon atoms and radicals attached to the edges of these species, and when they became large enough, they closed into hollow caged structures. While the bowl-shaped species have not been identified, planar graphitic sheets[11] appeared at about C_{29}^+ [8,11] and continued to about C_{60}^+. Even if these structures were to be reassigned to the bowl-shaped five- and six-member ring compounds,[12] it still would not explain why they suddenly appear at C_{29} or why the fullerenes suddenly appear at C_{30}.

The appearance of both species is likely due to collisional annealing[13] of large planar ring systems.[14,15] When planar rings larger than C_{35}^+ are injected into the mobility cell at high energy, they are converted nearly quantitatively to fullerenes, often with the loss of a small carbon radical to cool them.[14] These results provide an alternate growth model to radical addition to carbon bowl edges for fullerene formation in laser-induced plasmas or in carbon arcs. A recent summary and critique of the various carbon growth models has been given by Goroff.[16]

The annealing experiments indicated that carbon growth in laser plasmas is kinetically controlled.[14,15] Hence, a possible

[⊗] Abstract published in *Advance ACS Abstracts,* February 15, 1997.

S1089-5639(96)03140-4 CCC: $14.00

reason that the five- and six-member rings species are not observed could simply be kinetics: i.e., chains easily isomerize to rings, and these rings simply coalesce to form families of "ring" dimers, trimers, etc. The barriers to isomerization from these planar rings to bowls might be very high, and species energized to that level might simply decompose to smaller rings or chains.

One way to stabilize carbon is to chemically tie up the dangling bonds. When this is done with hydrogen, small five- and six-member ring species result, the important polycyclic aromatic hydrocarbon (PAH) class of compounds. Hence, one strategy is to add a small amount of hydrogen to the plasma forming the carbon clusters and try to identify structural change by the appearance or disappearance of "magic" cluster peaks (i.e., peaks with enhanced intensity relative to their neighbors). A number of such studies have been reported[17,18] with the general observations that clustering is reduced as the fraction of hydrogen is added and that some of the new hydrogenated peaks formed appear to have the right masses to be PAH components.[17,19] However, because the reacting system is so complex, it was generally not possible to follow the evolution of a specific PAH as hydrogen was added, and little could be said about the onset of PAH formation as sequential H-atoms were added to a carbon cluster of a given size.

In our first attempt at forming and identifying carbon rich PAH-like compounds, we chose to take a different approach. We started with decachloroacenaphthalene, $C_{12}Cl_{10}$, a per-chlorinated PAH with two fused six-member rings and a bridging five-member ring.[20] Experiments by Lifshitz, Grütz-macher, and co-workers[21] had indicated that these species would form relatively intense beams of C_n^+ ions when subjected to electron impact. Our strategy was to follow the structural changes in $C_{12}Cl_x^+$ as sequential Cl atoms were lost using IC techniques. We found that the $C_{12}Cl_{10}^+$ species could lose up to six Cl atoms and still retain the initial PAH structure. The $C_{12}Cl_3^+$ ion was too low in abundance to study. However, $C_{12}Cl_2^+$ and $C_{12}Cl_1^+$ turned out to be linear and C_{12}^+ a monocyclic ring. The latter result was consistent with the laser-induced plasma result on pure carbon.[8] Apparently, one Cl atom is sufficient to stabilize the linear structure and prevent it from closing to the monocyclic ring, at least under our experimental conditions.

In this paper we report results obtained when a small amount of hydrogen is added to the He expansion gas in our laser desorption ion source. Our goal was to follow structural evolution of the carbon clusters as H atoms are sequentially added. Structural determination on the resulting $C_nH_x^+$ ions was made for $9 \le n \le 22$ and $0 \le x \le 5$. The results obtained are compared to previous C_nH_x data in the literature. The relative ability of H atoms and electrons to stabilize dangling bonds is also discussed, and inferences are made on the relative abundances of neutral linear and cyclic isomers in the size range $10 \le n \le 20$.

The paper is organized as follows. First, a brief discussion of the experimental method is given followed by the experimental results. A discussion section follows, and a conclusion section summarizes the findings.

Experiment

The details of the apparatus have been given elsewhere[8,22] and will only be briefly recounted here. Ions are formed in a Smalley type laser desorption source, utilizing a XeCl excimer laser at 308 nm focused onto a graphite rod. The firing of the laser is synchronized with the opening of a pulsed valve with 5.45 atm backing pressure composed of 90% He and 10% H_2.

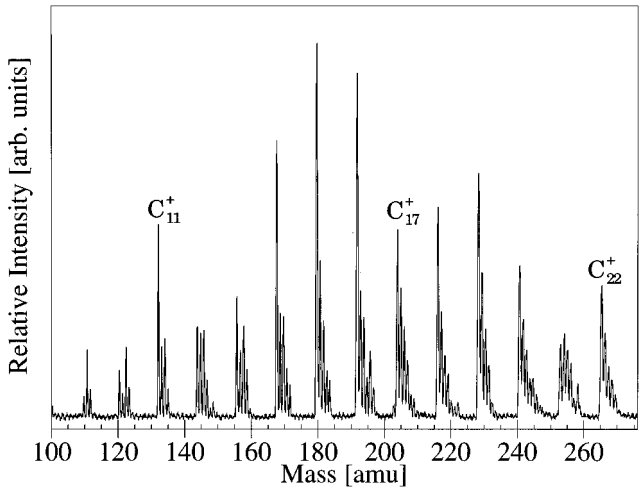

Figure 1. Mass spectrum of $C_nH_x^+$ species emanating from a laser desorption source with an expansion gas 90% He and 10% H_2.

The high-pressure gas pulse entrains the carbon plasma caused by the laser shot, travels 3−8 mm in a 2 mm diameter channel, and then expands into vacuum via a 30° conical nozzle. The entire source is floated at +5 kV. The beam passes through a skimmer, and the positively charged cluster ions are accelerated to ground potential and mass selected by a double-focusing reverse geometry mass spectrometer. At this point, either a mass spectrum can be obtained at an off-axis detector or a chosen mass-selected cluster ion can be decelerated, focused, and injected through a 0.5 mm hole at low laboratory energy (usually 5−30 eV) into a 4 cm long cell containing 5 Torr of He gas. Before entering the cell the ion beam is "clipped" by an electronic gate to a pulse 2 μs wide. Inside the cell the ion packet is subjected to a small drift field (2−20 V/cm). The ions exit via a 0.5 mm hole and pass through a quadrapole mass filter, and an arrival time distribution (ATD) is recorded at an electron multiplier detector using ion counting methods. All experiments reported here were done at 300 K.

Results

A typical mass spectrum is given in Figure 1 for an expansion gas mix of 90% He and 10% H_2. The spectrum continues to about $C_{40}H_x^+$ before intensities become too low to detect. For an expansion with 100% He the spectrum continues well above C_{120}^+. Satellite peaks are observed at 1 amu separation above the pure $^{12}C_n^+$ peak. These are predominantly due to sequential H atom addition, but the 1.13% ^{13}C isotope also contributes (typically 20−30%). The spectrum is shown only from $C_9H_x^+$ through $C_{22}H_x^+$ since this is the range being investigated in the work reported here. There are 3−6 H atoms added to the carbon clusters with the number of H atoms added generally increasing with carbon number.

A typical family of ATDs is given in Figure 2 for $C_{16}H_x^+$ for $0 \le x \le 5$. Similar families of ATDs were obtained for all clusters from $C_9H_x^+$ to $C_{22}H_x^+$. The C_{16}^+ ATD shows a single narrow peak indicating only a single structural isomer is present in the beam.[8] The $C_{16}H^+$ ATD is dominated by a single peak with approximately the same arrival time as C_{16}^+, but there is a small shoulder about 25 μs to longer times. For $C_{16}H_2^+$ this longer time shoulder is nearly as intense as the "original" shorter time peak and dominates the shorter time peak for $C_{16}H_3^+$. In $C_{16}H_4^+$ a new feature is observed about 15 μs to shorter times than the original peak, and this new feature has become much larger for $C_{16}H_5^+$.

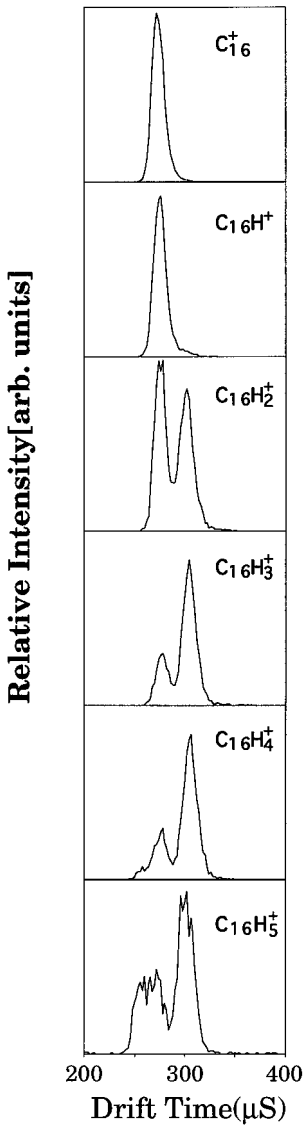

Figure 2. Arrival time distribution for $C_{16}H_x^+$ for $0 \le x \le 5$. The peak at longest times is due to the linear isomer ($n \ge 1$), that at shortest times a bicyclic isomer ($n \ge 4$), and the peak at intermediate times the monocyclic isomer ($n \ge 0$).

Discussion

Mobility Measurements. ATDs of the type shown in Figure 2 can be readily converted to ion mobilities, K, using eq 1.

$$v_d = KE \tag{1}$$

where v_d is the (measured) ion drift velocity and E is the electric field experienced by the ion in the drift cell. Kinetic theory[23] yields a form for the mobility at STP, K_0

$$K_0 = \frac{3q}{16N_o}\left[\frac{2\pi}{\mu k_b T}\right]^{1/2}\left[\frac{1}{\Omega^{(1,1)}(T)}\right] \tag{2}$$

where q is the ion charge, N_0 the gas number density at STP, μ the reduced mass, k_b Boltzmann's constant, T the absolute temperature, and $\Omega^{(1,1)}(T)$ the collision integral. If $\Omega^{(1,1)}(T)$ can be specified for a particular model structure, then mobilities for model structures can be compared to experimental mobilities and structural information obtained. The simplest method for specifying $\Omega^{(1,1)}(T)$ is to assume that the carbon cluster ion and the He collision partner undergo hard-sphere collisions. In this instance

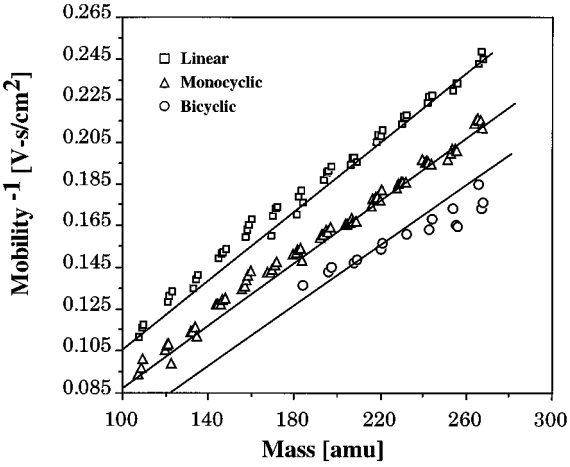

Figure 3. A plot of the inverse mobility vs mass for $C_nH_x^+$ species with $9 \le n \le 22$ and $0 \le x \le 5$ obtained from data like that shown in Figure 2. The lines are taken from earlier work on pure carbon and represent linear, monocyclic, and bicyclic structural isomers from top to bottom, respectively, allowing the same assignments to be made to the $C_nH_x^+$ species (see text).

$$\Omega^{(1,1)}{}_{HS} = \pi r_{HS}{}^2 \tag{3}$$

where r_{HS} is one-half the separation between the closest carbon nucleus of the cluster and the nucleus of the colliding He atom. This method has been shown to give excellent results for pure carbon clusters,[8,9] using a single value of r_{HS} approximately equal to the value obtained from van der Waals radii. While more sophisticated models are required to understand the variation of mobilities with temperature,[24,26] the hard-sphere model is sufficient to extract the structural information of interest to us here.

The data from ATDs like those in Figure 2 can be readily converted to K_0 values. We have found from experience that a useful way to display the data is to plot K_0^{-1} vs mass, since K_0^{-1} is approximately proportional to cross section. When data are plotted in this way, families of structures appear as quasi-linear progressions as cluster size (or mass) increases.[8,9] The K_0^{-1} data generated from the ATDs are plotted in Figure 3. It is apparent that three families of structures are involved. It is also clear that adding additional H atoms has only a minor affect on K_0^{-1} (i.e., on $\Omega^{(1,1)}{}_{HS}$). The lines drawn through the points are taken directly from our earlier work on pure carbon clusters.[8,9] The top line (largest K_0^{-1} values) corresponds to linear pure carbon clusters, and the middle line corresponds to monocyclic pure carbon clusters. It is obvious that identical assignments hold for the partially hydrogenated clusters represented by the corresponding data points in Figure 3. Hence, the ATDs at longest times in Figure 2 are due to linear chains, while those at intermediate times to monocyclic rings.

The line through the points at smallest K_0^{-1} is extrapolated from planar bicyclic rings in pure carbon clusters (which do not appear until C_{21}^+). There is qualitative agreement with the data points in Figure 3, but the slope is somewhat different. It should be noted the clusters giving these data points in Figure 3 contain at least four H atoms and first appear at $C_{15}H_4^+$. This point has important structural implications which we will come back to shortly. For now, it is reasonable to assign the peaks at shortest times in the ATDs, that appear only after four H atoms are attached, to some type of bicyclic planar ring.

Conformation and Hydrogenation. Traditionally, we have assigned conformations to clusters having a particular mobility

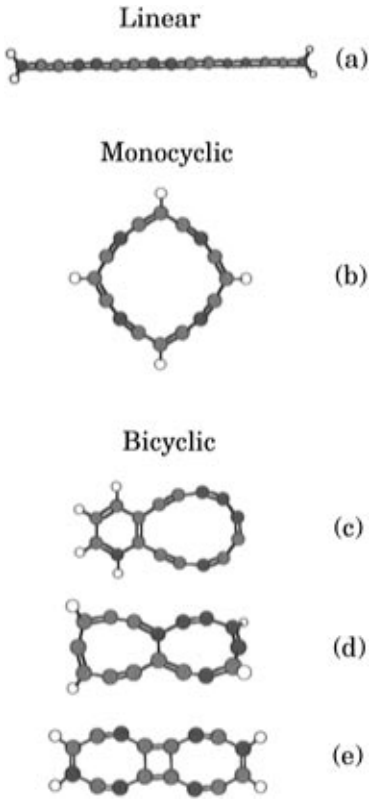

Figure 4. Possible structures of $C_{16}H_4^+$ isomers responsible for the ATD's in Figure 2 (see Table 1).

TABLE 1: Mobilities and Heats of Formation of Various $C_{16}H_4^+$ Isomers

			mobility (V cm^2 s^{-2})	
structure	isomer[a]	ΔH_f (kcal/mol)	exp	model
linear	**a**	440	5.21	5.10
monocyclic ring	**b**	580	6.19	6.35
bicyclic ring	**c**	350	6.98	6.75
	d	410	6.98	6.86
	e	410	6.98	6.70

[a] These letters correspond to the various structures in Figure 4.

(i.e., cross section) by generating model structures using theoretical methods. Rotationally averaged collision cross sections can be generated from these model structures using well-established methods.[8] We chose the semiemperical PM3 parametrization[27] found in the GAMESS[28] suite of programs to generate the model structures. Experience[8] has indicated that PM3 gives excellent 0 K structures of carbon clusters. The relative energies should be reliable as well (±20 kcal/mol), which will be important in identifying the structure of the bicyclic component.

Selected structures for the $C_{16}H_4^+$ molecules are given in Figure 4. The mobility and energetic information on these structures are collected in Table 1. Only a single isomer is shown as a representative for the linear family. Double hydrogenation of both terminal carbons is by far the lowest energy linear isomer leading to a cumulenic π-bonding arrangement. For $C_{16}H_2^+$ the linear form has a single hydrogen on each terminal carbon, and the chain is acetelynic. Preference for double hydrogenation of carbon clusters in this size range for clusters with an even number of carbon atoms was first shown by Heath et al.[17] and was interpreted in terms of polyacetelynic chains.

There are many possible isomers for the monocyclic ring family of nearly the same energy, and only the quasi-square symmetric structure is shown. Each of these isomers has relatively high energy, according to PM3 calculations, which probably accounts for the small amount of this species relative to the more stable linear isomer (Figure 2).

$C_{16}H_4^+$ is composed of ~10% bicyclic ring. In pure carbon bicyclic rings did not occur until $n > 20$, and the almost certain mechanism of formation was coalescence of two monocyclic rings each with $n \geq 10$. It is exceedingly unlikely that the $C_{16}H_4^+$ bicyclic ring observed here resulted from the coalescence of two $C_8H_2^+$ monocyclic rings since all hydrogenated $C_8H_x^+$ species in our experiments are linear (even though the data are not shown here). Since pure carbon bicyclic rings do not exist in this size range, they cannot be directly hydrogenated. Hence, these new species arise from new chemistry occurring both in the laser-induced plasma and in subsequent reactivity downstream.

Three examples of possible "bicyclic" species are given in Figure 4 and in Table 1. Based on mobility alone, structure **d** agrees slightly better with experiment than **c** and **e**, although all are within the acceptable range. This agreement is misleading, however, as these are 0 K model mobilities, but the experiments occurred at 300 K. Unfortunately, we cannot obtain 300 K averaged structures using PM3, since it is not set up to do dynamics, but it appears reasonable that thermal motion will induce out-of-plane bending and reduce the average size of all three bicyclic structures and hence increase their mobility by a few percent.

Thermochemistry strongly favors structure **c**. This is essentially a benzene ring with an attached C_{10} loop. This structure makes some sense because the bicyclic family did not appear until four H atoms were attached to the carbon cluster, which allows formation of the stable ortho-substituted benzene moiety. Also, $C_{15}H_4^+$ is the smallest cluster exhibiting a bicyclic isomer, probably because at least nine atoms are required in the carbon loop to minimize ring strain.

In earlier studies Heath et al.[17] found that at low H_2 fractions in the He buffer gas used in their laser desorption souce $C_nH_2^+$ was a favored species for $n = 10$, 12, 14, and 16 while $C_nH_6^+$ was a favored at relatively high H_2 fractions. They rationalized their results in terms of initial hydrogenation of the two terminal carbon atoms in a linear chain followed by complete hydrogenation of a triple bond.

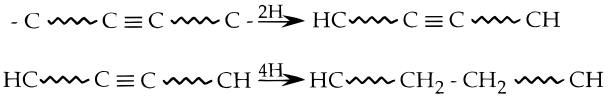

A second hydrogenation mechanism that leads to formation of PAHs, which are observed under hydrogen saturation conditions at larger sizes,[19] is generation of structures like those given below.

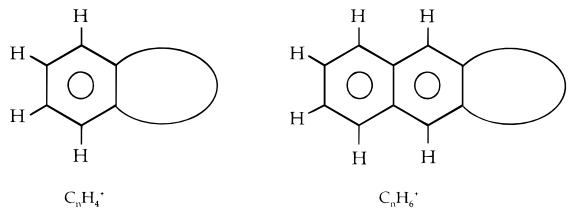

Heath et al.[17] also observed what appeared to be magic numbers for 10 H atom additions for $n > 14$ at highest H_2 partial pressures. The number of possibilities for these structures is large and may include staturation of one or more of the aromatic rings.

DeVries et al.[19] laser-ablated graphite in a static chamber at 500 Torr total pressure and collected samples of the soot formed

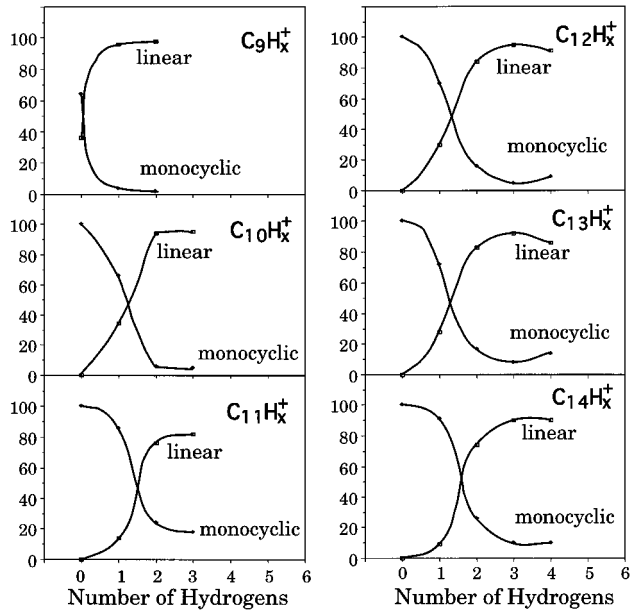

Figure 5. Fractional isomer abundances for $C_nH_x^+$ for $9 \leq n \leq 14$ and $0 \leq x \leq 4$ determined from ATDs analogous to those shown in Figure 2.

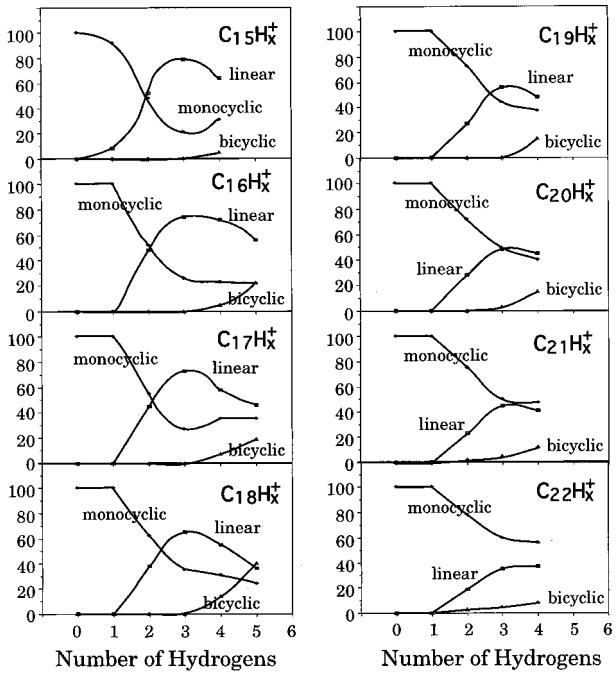

Figure 6. Fractional isomer abundances for $C_nH_x^+$ for $15 \leq n \leq 22$ and $0 \leq x \leq 5$ determined from ATDs analogous to those shown in Figure 2.

from deposition of ablated carbon on surfaces at room temperature. A unique two-laser, jet cooling, time of flight analysis was done on the soot deposits. With pure He as the bath gas the soot was shown to have a broad distribution of C_n^+ peaks with $n \geq 56$ and dominated by $n = 60$. These peaks were reasonably assigned as fullerenes. When a small (0.4%) amount of H_2 was present, a new series of peaks appeared at masses of 354 amu and below ($n \leq 27$) that nearly equaled the fullerenes in integrated intensity. With 10% H_2 in the buffer gas only the low mass species were observed. Prominent features in this low mass spectrum correlated with common PAH masses and were so assigned. This data clearly shows that H_2 quenches clustering of carbon and completely removes the precursors required for fullerene formation. It also strongly suggests that PAHs are prominent among the products formed.

It would, of course, be very interesting to follow the structural evolution of carbonecious species as H atoms are attached. A summary of the results we have obtained up to $C_{22}H_5^+$ is given in Figures 5 and 6. At small carbon sizes (up to $n = 14$, see Figure 5) only the linear and monocyclic ring species are present. For pure carbon cations, monocyclic rings make up ~100% of the ionization for $n \geq 10$. In all cases $C_nH_1^+$ species are at least partly linear, ranging from ~100% at $n = 9$ to ~10% at $n = 14$. For $C_nH_2^+$, however, the linear isomer totally dominates for all values of n. Heath et al.[17] ascribed $C_nH_2^+$ (n = even) magic numbers to polyacetylene formation. This suggestion is most likely correct for n even

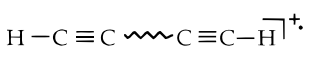

(n = even)

but cannot be true for n odd, where cumulenic structures should dominate. In this case there are (at least) two possibilities:

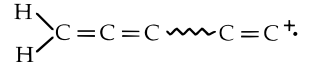

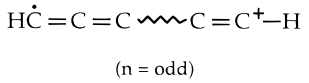

(n = odd)

The top cumulenic structure is a "classical" radical cation, while the bottom is an example of the more recently discovered "distonic" radical cation where the charge and radical centers are formally separated. Of course, due to symmetry, the two resonance forms of the distonic radical cation mix leading to the charge and radical sites being developed on both ends. Semiemperical calculations using the PM3 parametrization indicate that for n = even the neutral polyacetylene form with H atom capping at each end is more stable by 100 kcal/mol than the isomer with both H atoms located on the same terminal carbon. The same stability ordering holds in the cations and anions, but the difference in energy is reduced to 50 and 20 kcal/mol, respectively. Similar results hold for n = odd, except the energy differences are reduced somewhat.

At $n \geq 15$ two changes occur (Figure 6). For $C_nH_2^+$, linear and monocyclic forms effectively compete with monocyclic rings dominating by $n = 19$. In this size range C_nH^+ species are 100% monocyclic. For $C_nH_3^+$ and $C_nH_4^+$ linear species again are prevalent until $n = 21$ where monocyclic rings emerge as the most abundant isomer. Reactivity studies by Böhme and Wlodek[29] indicate C_n^+ ions for $n < 10$ react relatively quickly with H_2 in a flow tube forming primarily $C_nH^+ + H$ products, but C_n^+ ions for $n \geq 10$ are completely unreactive with H_2. These results are interpreted to mean monocyclic rings do not react with H_2, but linear chains do, conclusions consistent with a number of earlier reactivity studies[30] done using FT-ICR. It is clear from the large number of studies on carbon cluster formation in laser desorption sources that reactivity not only occurs in the laser plume but also continues down the flow channel until exiting the nozzle. It also seems reasonable that carbon cations will be much more reactive with H_2 (or H) than carbon neutrals, as entrance channel barriers will be greatly reduced. Since linear chains dominate in pure carbon with $n < 10$, these species will attack H_2 and form $C_nH_x^+$ linear species. That this is so is clear from Figures 1 and 5. For $n = 9$ the dominant peak is C_9H^+, and for $n = 10$ it is $C_{10}H_2^+$. For $n \geq 11$, however, the pure carbon component dominates for every carbon number except $n = 21$, probably reflective of the greatly reduced reactivity of monocyclic rings with H_2. The multiply

hydrogenated species in this size range are due primarily to the reaction of H atoms and small carbon radicals with monocyclic rings.

In the $C_{12}Cl_x^+$ work[20], it was found that C_{12}^+ was 100% monocyclic ring; $C_{12}Cl^+$ and $C_{12}Cl_2^+$ were 100% linear; and $C_{12}Cl_4^+$ was 70% graphitic (i.e., PAH like), 22% monocyclic ring, and 8% linear. These species were formed by electron impact on $C_{12}Cl_{10}$, decachloroacenaphthene, a tricyclic molecule with a five-member ring bridging the two fused benzene rings that make up the naphthalene backbone. By comparison, when $C_{12}H_x^+$ is made under our reaction conditions, C_{12}^+ is 100% monocyclic ring; $C_{12}H^+$ is 70% monocyclic and 30% linear; $C_{12}H_2^+$, $C_{12}H_3^+$, and $C_{12}H_4^+$ are 10 ± 5% monocyclic and 90 ± 5% linear. There is no evidence for either a bicyclic or graphitic isomer. The relative stabilities of the various structures are similar, whether Cl or H is stabilizing the dangling bond. Hence, the relative abundances observed in our experiments, as well as in essentially all other experiments done to date, depend on the formation pathways available in the experiments and do not necessarily mirror the thermodynamic stability of the various species. While this is not a particularly surprising result, it requires that caution be used in either drawing structural conclusions from magic numbers in mass spectra (a very common practice) or in drawing conclusions on isomeric stability from a single set of structural determinations.

Annealing measurements of the type done on larger carbon rings[14,15] offer one type of check on the structure/stability relationship. However, since isomerization barriers often exceed dissociation energies, it is very useful to attempt to approach the problem from a separate point on the potential energy surface as we did in the $C_{12}Cl_{10}$ work.

Dangling Bonds. The question of the importance of dangling bonds on carbon in dictating structure can be looked at in the following way. Consider the linear to ring transition in carbon:

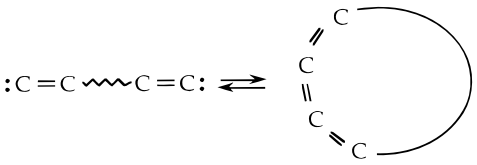

The two forces that determine the direction of this simple equilibrium are generated by bond formation and ring strain. Linear to cyclic bond formation eliminates the dangling bonds but forces the system into a nonlinear configuration, which in pure carbon induces ring strain.

Addition of stabilizing elements tends to favor the linear over the monocyclic ring since the energy released by bond formation decreases more than the ring strain decreases. Two kinds of stabilizing agents can be added: the first is simply electrons, and the seconds is an electron donor radical like the H atom. These two types of donors are compared in Figure 7.

In Figure 7a the percentage of linear isomer is plotted vs cluster size for $5 \geq n \geq 20$ for both C_n^+ and C_n^-. In both instances the clusters were generated by laser desorption of graphite. In order to remove effects of differential reactivity of the linear and cyclic isomers, both the cation[8c,d] and anion[9b] clusters were annealed.[13] These annealed results are plotted in Figure 7a.

The anions are essentially 100% linear up to $n = 12$, but this fraction monotonically falls off above $n = 12$, reaching ~5% by $n = 20$ (and totally disappearing at $n = 30$).[9] The only other isomer observed in this size range is the monocyclic ring. In contrast, the cations are 100% linear for $n = 5$ and 6, fall to 20 ± 10% linear for $n = 7-10$, and then have essentially no

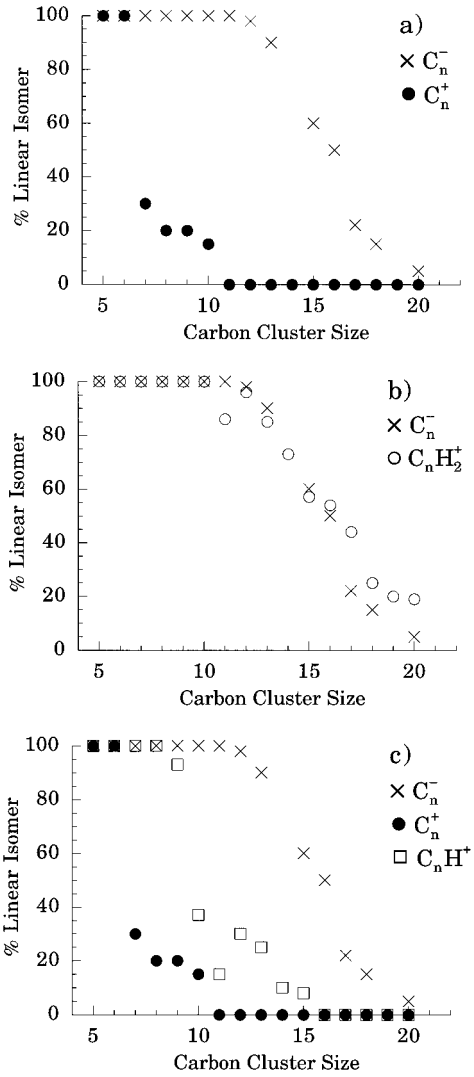

Figure 7. Plots of the percent linear isomer abundance vs the carbon cluster size, *n*, for (a) C_n^+ and C_n^-, (b) C_n^- and $C_nH_2^+$, and (c) C_n^+, C_nH^+, and C_n^-.

linear isomer present for $n \geq 10$. The driving force for bond formation and the resistance due to ring strain compete for $n = 7-10$ for the cations with ring strain clearly winning below $n = 7$ and bond formation clearly winning above $n = 10$. The shift to larger cluster size in the anions before ring closure occurs and the much more gradual falloff in the linear isomeric percentage with cluster size are consistent with a much smaller driving force for bond formation (due to the two extra electrons in the anions satisfying dangling bonds present in the cations), while ring strain remains more or less constant.

A second interesting comparison is given in Figure 7b. Here, the linear isomer percentages of the C_n^- anions and the $C_nH_2^+$ cations are compared as a function of cluster size. If H atoms are simply electron donors, then the two systems should behave approximately the same. The agreement between the two sets of data is remarkably good (especially since strict isomer equilibria were not experimentally obtained). In this range only linear and monocyclic ring isomers are possible for these two systems, and their interconversion is a relatively simple process. Hence, it can be stated with some confidence that the data in Figure 7 dramatically illustrate the importance of dangling bonds in driving structural change in small carbon clusters. They also indicate that, to a surprising extent, H atoms can be considered simply as electron donors tying up dangling bonds.

These data are consistent with ab initio calculations[8e] on C_7^+, C_7, and C_7^-. These calculations indicate the cyclic form of C_7^+ is 0.75 eV more stable than the linear, but for neutral C_7 the linear isomer is 1.12 eV more stable than the cyclic, and for the anion the linear form is 2.11 eV more stable than the cyclic.

If adding two H atoms effectively mimics structural changes in going from C_n^+ to C_n^-, then it is not unreasonable that the addition of a single H atom would mimic structural change in going from C_n^+ to neutral C_n. The linear percentages of C_nH^+ are plotted in Figure 7c vs cluster size, along with the C_n^+ and C_n^- data for comparison. Not unexpectedly, these data "split the difference" between the C_n^+ and C_n^- data and provide the first insight into neutral carbon cluster structural distributions in this size range. Spectroscopic evidence for the n = odd neutral linear isomers in the gas phase have been found up to $n = 13$, and their possible importance in the chemistry of the interstellar medium has been discussed.[31] If our interpretation of the data given in Figure 7c is correct, then spectroscopic detection of linear C_{15} will be experimentally difficult, and higher order linear clusters will not exist. Unfortunately, spectroscopic methods have not yet been developed to observe neutral monocyclic clusters which we predict to dominate above $n = 10$.

Conclusions

The basic findings of this work are as follows:

1. Addition of hydrogen to the helium expansion gas in a laser desorption source substantially reduces clustering and essentially eliminates fullerene formation.

2. The dominant isomers present for $n = 5-22$ are linear and monocyclic ring. Addition of H atoms has the effect of extending the linear isomer range to larger values of n at the expense of the cyclic fraction.

3.The first evidence of a species related to PAH formation appears at $C_{15}H_4^+$, which appears to be a benzene ring with a carbon loop attached to ortho positions. This bicyclic species increases in fractional abundance as n increases and always requires at least four H atoms. The first "bicyclic" species in pure carbon appears at $C_{21}+$ and is composed of two coalesced monocyclic rings.[8]

4.The fractional abundances of $C_nH_2^+$ and C_n^- linear and monocyclic ring isomers quantitatively agree from $n = 5$ to $n = 20$, indicating H atoms primarily act as single electron donors as far as structure is concerned. It is argued that the C_nH^+ isomer abundances should then mirror the neutral C_n abundances, providing the first experimental estimates of these important but elusive quantities.

Acknowledgment. The support of the Air Force Office of Scientific Research under Grant F49620-96-10033 and the partial support of the National Science Foundation under Grant CHE-9421176 are gratefully acknowledged.

References and Notes

(1) Honig, R. E. *J. Chem. Phys.* **1954**, *22*, 126. Hinterberger, H.; Franzen, J.; Schuy, K. D. *Z. Naturforsch. A* **1963**, *18*, 1236. Leleyter, M.; Jones, P. *Radiat. Eff.* **1973**, *18*, 105. Weltner, Jr., W.; van Zee, R. J. *Chem. Rev.* **1989**, *89*, 1713 and references therein.

(2) Kroto, H. W.; Heath, J. R.; O'Brien, S. C.; Curl, R. F.; Smalley, R. E., *Nature* **1985**, *318*, 162. Zhang, Q. L.; O'Brien, S. C.; Heath, J. R.; Liu, Y.; Curl, R. F.; Kroto, H. W.; Smalley, R. E. *J. Phys. Chem.* **1986**, *90*, 525.

(3) Kratschmer, W.; Fostiropoulos, K.; Huffman, D. R. *Chem. Phys. Lett.* **1990**, *170*, 167. Meijer, G.; Bethune, D. S. *Chem. Phys. Lett.* **1990**, *175*, 1. Haufler, R. E.; Conceicao, J.; Chibante, L. D. F.; Chai, Y.; Byrne, N. E.; Flanagan, S.; Haley, M. M.; O'Brien, S. C.; Pan, C.; Xiao, Z. Billups, W. E.; Cuifolini, M. A.; Hauge, R. H.; Margrave, J. L.; Wilson, L. J.; Curl, R. F.; Smalley, R. E. *J. Phys. Chem.* **1990**, *94*, 8634. Diederich, F.; Ettl, R.; Rubin, Y.; Whetten, R. L.; Beck, R.; Alverez, M.; Ang, S.; Sensharma, D.; Wudl, F.; Khemani, K. C.; Koch, A. *Science* **1991**, *252*, 548. Taylor, R.; Hare, J. P.; Abdulsada, A. K.; Kroto, H. W. *J. Chem. Soc., Chem. Commum.* **1990**, *N20*, 1423.

(4) Iijima, S. *Nature* **1991**, *354*, 56. Ugarte, D. *Nature* **1992**, *359*, 707. Johnson, R. D.; deVries, M. S.; Salem, J. R.; Bethune, D. S.; Yannoni, C. S. *Nature* **1992**, *355*, 239. Iijima, S.; Ichihashi, T. *Nature* **1993**, *363*, 603. Bethune, D. S.; Keang, C. H.; deVries, M. S.; Gorman, G.; Savoy, R.; Vazques, J.; Beyers, R. *Nature* **1993**, *363*, 605.

(5) Heath, J. R.; O'Brien, S. C.; Zhang, Q.; Liu, Y.; Curl, R. F.; Kroto, H. W.; Tittle, F. K.; Smalley, R. E. *J. Am. Chem. Soc.* **1988**, *110*, 4464. Kikuchi, K.; Suzuki, S.; Nakao, Y.; Nakamura, N.; Wakabayashi, T.; Shiromanu, H.; Saito, K.; Ikemoto, I.; Achiba, Y. *Chem. Phys. Lett.* **1993**, *216*, 67. McElvaney, S. W. *J. Phys. Chem.* **1992**, *96*, 4935. Clemmer, D. E.; Shelminov, K. B.; Jarrold, M. F. *Nature* **1994**, *367*, 718.

(6) Kemper, P. R.; Bowers, M. T. *J. Am. Chem. Soc.* **1990**, *112*, 3231; *J. Phys. Chem.* **1991**, *95*, 5134. Bowers, M. T.; Kemper, P. R.; von Helden, G.; van Koppen, P. A. M. *Science* **1993**, *260*, 1446.

(7) Lee, S.; Gotts, N. G.; von Helden, G.; Bowers, M. T. *Science* **1995**, *267*, 999.

(8) (a) von Helden, G.; Hsu, M.-T.; Kemper, P. R.; Bowers, M. T. *J. Chem. Phys.* **1991**, *95*, 3835. (b) von Helden, G.; Hsu, M.-T.; Gotts, N. G.; Bowers, M. T. *J. Phys. Chem.* **1993**, *97*, 8182. (c) von Helden, G.; Gotts, N. G.; Bowers, M. T. *Chem. Phys. Lett.* **1993**, *212*, 241. (d) von Helden, G.; Gotts, N. G.; Palke, W. E.; Bowers, M. T. *Int. J. Mass Spectrom. Ion Processes* **1992**, *138*, 33. (e) von Helden, G.; Palke, W. E.; Bowers, M. T. *Chem. Phys. Lett.* **1993**, *212*, 247.

(9) (a) von Helden, G.; Kemper, P. R.; Gotts, N. G.; Bowers, M. T. *Science* **1993**, *259*, 1300. (b) Gotts, N. G.; von Helden, G.; Bowers, M. T. *Int. J. Mass Spectrom. Ion Processes* **1995**, *149/150*, 217.

(10) Heath, J. R.; O'Brien, S. C.; Curl, R. F.; Kroto, H. W.; Smalley, R. E. *Comments Condens. Matter Phys.* **1987**, *13*, 119. Smalley, R. E. *Acc. Chem. Res.* **1992**, *25*, 98.

(11) Shelminov, K. B.; Hunter, J. M.; Jarrold, M. F. *Int. J. Mass Spectrom. Ion Processes* **1994**, *138*, 17.

(12) Shvartsburg, A. A.; Jarrold, M. F. *Chem. Phys. Lett.* **1996**, *261*, 86.

(13) Jarrold, M. F.; Honea, E. C. *J. Am. Chem. Soc.* **1992**, *114*, 459.

(14) von Helden, G.; Gotts, N. G.; Bowers, M. T. *Nature* **1993**, *363*, 60; *J. Am. Chem. Soc.* **1993**, *115*, 4363.

(15) Hunter, J. M.; Fye, J. L.; Jarrold, M. F. *Science* **1993**, *260*, 784. Hunter, J. M.; Fye, J. L.; Roskamp, E. J.; Jarrold, M. F. *J. Phys. Chem.* **1994**, *98*, 1810.

(16) Goroff, N. *Acc. Chem. Res.* **1996**, *29*, 77.

(17) Heath, J. R.; Zhang, Q.; O'Brien, S. C.; Curl, R. F.; Kroto, H. W.; Smalley, R. E. *J. Am. Chem. Soc.* **1987**, *109*, 359.

(18) Rohlfing, E. A. *J. Chem. Phys.* **1990**, *93*, 7851. Allaf, A. W.; Hallett, R. A.; Bohn, S. P.; Kroto, H. W. *Int. J. Mod. Phys. B* **1992**, *6*, 3595. Doverstal, M.; Lindgren, B.; Sassenberg, U.; Yu, H. *Phys. Scr.* **1991**, *43*, 373.

(19) deVries, M. S.; Reiks, K.; Wendt, H. R.; Golden, W. G.; Hunzcker, H. E.; Fleming, R.; Peterson, E.; Chang, S. *Geochim. Cosmochim. Acta* **1993**, *57*, 933.

(20) von Helden, G.; Porter, E.; Gotts, N. G.; Bowers, M. T. *J. Phys. Chem.* **1995**, *99*, 7707.

(21) Lifshitz, C.; Peres, T.; Agrarat, I. *Int. J. Mass Spectrom. Ion Processes* **1989**, *93*, 149. Sun, J.; Grützmacher, H.-F.; Lifshitz, C. J. *J. Am. Chem. Soc.* **1993**, *115*, 8382. Sun, J.; Grützmacher, H.-F.; Lifshitz, C. *Int. J. Mass Spectrom. Ion Processes* **1994**, *138*, 49.

(22) Kemper, P. R.; Bowers, M. T. *J. Am. Soc. Mass Spectrom.* **1990**, *1*, 197.

(23) Mason, E. A.; McDaniel, E. W. *Transport Properties of Ions in Gases*; Wiley: New York, 1988.

(24) von Helden, G.; Wyttenbach, T.; Bowers, M. T. *Int. J. Mass Spectrom. Ion Processes* **1995**, *146*, 349.

(25) Wyttenbach, T.; von Helden, G.; Batka, J. J.; Carlat, D.; Bowers, M. T., *J. Am. Soc. Mass Spectrom.*, in press.

(26) Mesleh, M. F.; Hunter, J. M.; Shvartsburg, A. A.; Schatz; G. C.; Jarrold, M. F., *J. Phys. Chem.* **1996**, *100*, 16082.

(27) Steward, J. J. P. *J. Comput. Chem.* **1989**, *101*, 209.

(28) Schmidt, M. W.; Baldridge, K. K.; Boatz, J. A.; Elbert, S. T.; Gordon, M. S.; Jensen, J. H.; Koseki, S.; Matsunaga, N.; Nguyen, K. A.; Su, S. J.; Windus, T. L.; Dupuis, M.; Montgomery, J. A. *J. Comput. Chem.* **1993**, *14*, 1347.

(29) Böhme, D. K.; Wlodek, S. *Int. J. Mass Spectrom. Ion Processes* **1990**, *102*, 133.

(30) McElvany, S. W.; Dunlap, B. I.; O'Keefe, A. O. *J. Chem. Phys.* **1987**, *86*, 715. McElvany, S. W.; Creasy, W. R.; O'Keefe, A. O. *J. Chem. Phys.* **1986**, *85*, 632.

(31) Giesen, T. F.; Van Orden, A.; Hwang, H. J.; Fellers, R. S.; Provencal, R. A.; Saykally, R. J. *Science* **1994**, *265*, 22 and references therein.